

Scanning Probe Microscopy with Landmark Referenced Control for Direct Biological Investigations

B. Goolsby,^a Q. Chen,^a L. Udpa,^a Y. Fan,^a R. Samona,^a B. Bhooravan,^a
F. M. Salam,^a D. H. Wang,^b and V. M. Ayres^a

^aDepartment of Electrical and Computer Engineering, Michigan State University, East Lansing, Michigan 48824, USA

^bDepartment of Medicine, Michigan State University, East Lansing, Michigan 48824, USA

We report the successful use of continuous wavelet transforms applied to atomic force microscope data sets for landmark recognition of biological features. The data sets were images of mixed red and white blood cells. Contrast enhancement followed by continuous wavelet transform of the data was used to successfully distinguish erythrocytes from neutrophil and monocyte leukocytes within the mixed cell images. All of the above are spherical objects between 6 and 8 μm in diameter, which demonstrates the ability to sort similar biological objects into distinct classes. The implications for development of on-line scanning probe recognition microscopy are discussed.

Keywords: Scanning Probe Microscopy, Atomic Force Microscopy, Biological Systems, Cells, Image Processing, Continuous Wavelet Transform.

1. INTRODUCTION

Scanning probe microscopy (SPM) provides high-resolution imaging of specimens, including biological specimens. SPM-based nanomanipulation is a newly emerging area that offers an orders-of-magnitude improvement over current manipulation capabilities. Together, the two offer the possibility of site-specific direct investigations of biological events. Our group has developed a landmark recognition scheme for use within an adaptive nonlinear neural network controller, for high-end control of the X - Y motion of an SPM tip.¹⁻⁴ Such a specially equipped SPM can be used for direct site-specific investigations of particular nanobiological features and interactions.

In this paper, we present our recent research on landmark recognition of biological features. The data sets were atomic force microscope (AFM) images containing mixed erythrocytes (red blood cells) and leukocytes (white blood cells). Each image was a 512×512 pixel raster scan with three x - y - z points per pixel. Such large data sets are typical for AFM images. Contrast enhancement followed by continuous wavelet transform of the data set was used to successfully distinguish erythrocytes from neutrophil and monocyte leukocytes within the mixed cell images. All of the above are spherical objects between 6 and 8 μm in diameter.

2. EXPERIMENTAL DETAILS

2.1. Mixed Cell Type and AFM Data Set Acquisition

Blood samples (about 3 ml), from male Wistar rats (Charles River Laboratories, Wilmington, MA), were centrifuged at 300 rpm at 4 °C for 15 min. Small volumes (<1 ml) containing mainly neutrophilic leukocytes and a small amount of erythrocytes on top of the centrifuged samples were extracted with a pipette and placed on a glass cover slide. AFM images of the mixed cell types were obtained with a Digital Instruments Nanoscope IIIa operated in tapping mode in ambient air. Other experimental parameters included: use of a J scanner with a maximum $125 \times 125 \mu\text{m}^2$ x - y scan range, silicon tips with a nominal 10-nm tip radius of curvature, and a scan rate of approximately 1 Hz. The cells adhered readily to the glass slides, and there was no visible evidence of tip-induced damage to the samples.

A typical mixed cell image is shown in Figure 1. By inspection, it contains seven erythrocytes (red blood cells) and four leukocytes (white blood cells). In addition to the neutrophil leukocytes, identifiable by their crescent-shaped nucleus, an anomalous leukocyte is also observed. This is possibly a monocyte, a white blood cell that responds to chronic inflammation, as opposed to a neutrophil, a white blood cell that responds to acute inflammation. Therefore,

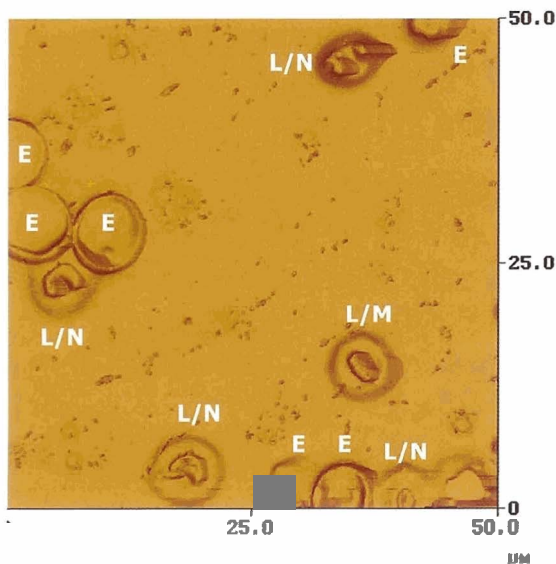


Fig. 1. A typical mixed cell image. The cells are: E-erythrocytes (red blood cells), L/N-leukocytes (white blood cells)/neutrophil type, and L/M-leukocyte (white blood cell)/possible monocyte type. All are spherical and about 6 to 8 μm in diameter.

there are eleven spherical objects in, or partly in, the image which are about 6 to 8 μm in diameter.

2.2. Recognition Using Continuous Wavelet Transform

The image data were first extracted in Height Plot type as opposed to Illuminate Plot type.⁵ In Height Plot type, the data are encoded with their height values only. A visual image of Height Plot type encoded data will represent the height values as a color table, as shown in Figure 2a. In Illuminate Plot type, which is the usual encoding of SPM data for the convenience of a human observer, the data are displayed as if a light source is shining on the sample surface from a selectable direction. This artificial lighting is unnecessary for the recognition algorithm. An image displayed in Height Plot type will look “murky” by comparison with an image displayed in Illuminate Plot type.

Next contrast enhancement was performed as a preprocessing step. In SPM the value of the z coordinate as a function of (x, y) is projected over a range from the

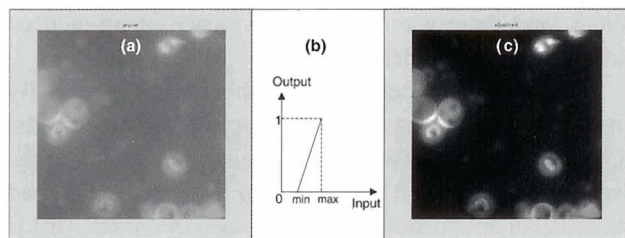


Fig. 2. (a) The initial data values, with artificial lighting removed. (b) Linear mapping to increase the contrast of the images. (c) Contrast enhanced image data used in subsequent processing.

lowest to highest value. Within an image, many z values may cluster within a limited subset of the full range. To increase the contrast of the image, the data values $z(x, y)$ were remapped to utilize the full dynamic range, using a linear mapping,

$$Z(x, y) = \frac{1 - 0}{\max(z(x, y)) - \min(z(x, y))} \times (z(x, y) - \min(z(x, y))) \quad (1)$$

An example is shown in Figure 2. The enhanced data sets were used in all subsequent processing steps.

Although contrast enhancement based on a statistical differencing filter⁶ is an available feature in the SPM, this paper implements a linear mapping for enhancing contrast of the raw image from the SPM. This allows inversion of the mapping to retrieve the height domain information and provides flexibility of choice of the contrast enhancement algorithm as appropriate for a particular data set.

A continuous wavelet transform is a scale based two-dimensional transformation that allows multiscale/multi-resolution analysis of images.^{7,8} The transformed data set $W(\sigma, \tau_1, \tau_2)$ is given by

$$W(\sigma, \tau_1, \tau_2) = \frac{1}{\sigma} \iint z(x, y) \psi^* \left(\frac{x - \tau_1}{\sigma}, \frac{y - \tau_2}{\sigma} \right) dx dy \quad (2)$$

where σ is the scale parameter, τ_1, τ_2 are the translation parameters, * denotes the complex conjugation, and ψ is the wavelet basis set derived from a mother wavelet⁸ $\hat{\psi}$. The scale parameter σ plays a crucial role. Wavelet transforms process data at different scales or resolutions. At each scale they compute the similarity of the image data with the wavelet kernel at the selected scale σ . At large scales, the transform coefficients $W(\sigma, \tau_1, \tau_2)$ are dominant for data from objects in the image that correspond to the larger scale wavelet kernel. Similarly, for small scales, small features are highlighted in the $W(\sigma, \tau_1, \tau_2)$ transform domain. By choosing the appropriate scale, we can get the relevant details from the image that are necessary to perform a particular recognition task across multiple scales. The resolution of the multiscale recognition technique corresponds to the resolution of the features within the image. This is nanometer scale for AFM images and angstrom scale for STM images.

The multiscale analysis procedure begins by defining a mother wavelet function $\hat{\psi}$. One candidate $\hat{\psi}$ is expressed as

$$\hat{\psi}(\sigma, x, y) = \frac{1}{\left\| \varphi \left(\frac{x^2 + y^2}{\sigma} \right) \right\|} \varphi \left(\frac{x^2 + y^2}{\sigma} \right) \quad (3)$$

where φ is a function used for systematic generation of images of slowly varying scale σ . A Gaussian is a commonly used function whose scale is determined by the variance σ . A multiscale edge detector can be derived from the spatial derivatives of φ .

Edges associated with abrupt transitions in the image were detected with a two dimensional multiscale Gaussian differential operator defined as

$$\vec{\psi}(x, y) = \frac{d\varphi(x, y)}{dx} \hat{i} + \frac{d\varphi(x, y)}{dy} \hat{j} \quad (4)$$

The scaled decomposition of the image can be performed by convolving the image data $Z(x, y)$ with the differential Gaussian wavelet parameterized by scale σ . For a fixed value of scale, we can calculate the 2D CWT in frequency domain,

$$W(\sigma, w_1, w_2) = \sigma Z(w_1, w_2) \Psi^*(\sigma w_1, \sigma w_2) \quad (5)$$

where Ψ is the Fourier Transform of ψ .

2.3. Analysis of AFM Data Sets

Analysis of the AFM data sets from several mixed cell images was performed by contrast enhancement followed by continuous wavelet transformation, with the scale parameter $\sigma = 6$. The horizontal and vertical cross sections of representative continuous wavelet transforms $W(\sigma, \tau_1, \tau_2)$ are shown in Figure 3 (the examples shown correspond to the cell types in Fig. 1 and

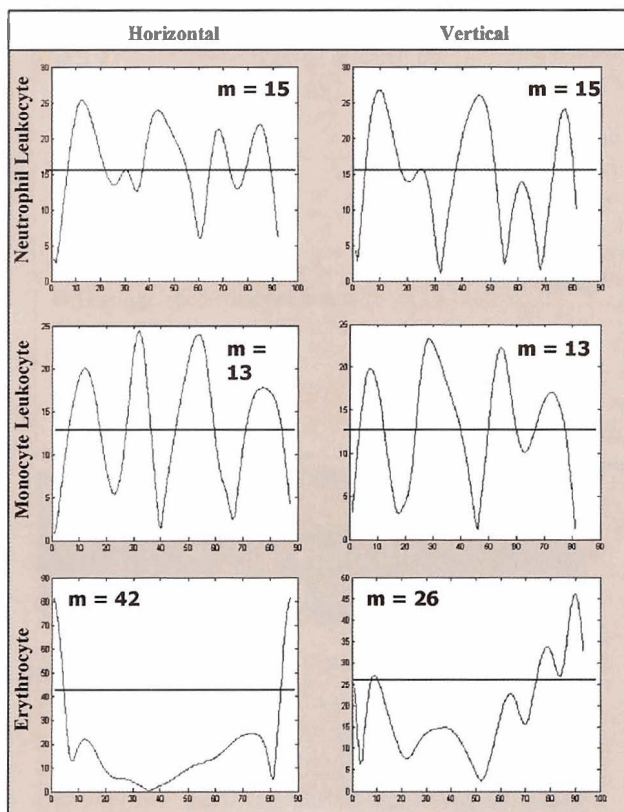


Fig. 3. Continuous wavelet transforms $W(\sigma, \tau_1, \tau_2)$ shown for horizontal ($y = 0$) and vertical ($x = 0$) axes. The mean value m is displayed for each plot. Number of zero crossing $n =$ number of times, the plot intersects the mean line. For all specimens studied, the number of zero crossings $n < 4$ corresponded to a red blood cell and $n > 4$ to a white blood cell.

are representative of all the others). After subtracting the mean value m from the cross-sectional plots in Figure 3, we can count the number of zero crossings n , which is seen to be indicative of the object type. In all images obtained from the blood samples described earlier containing mainly erythrocytes and neutrophilic leukocytes, erythrocytes could be identified by $n < 4$ zero crossings, and leukocytes by $n > 4$ zero crossings.

3. RESULTS AND DISCUSSION

Contrast enhancement followed by continuous wavelet transform of the data was used to successfully distinguish erythrocytes from neutrophil and monocyte leukocytes within the mixed cell images. All of the above are spherical objects about 6 to 8 μm in diameter, which demonstrates the ability of this algorithm to provide individual feature recognition among similar biological objects. We note that the continuous wavelet formulation also inherently contains the capability to extract multiple scales of features from the same object, through variation of the scale parameter σ . The limit of the scale resolution is the same as the pixelation of the SPM image, and it can be made even smaller through the use of sophisticated algorithms that offer subpixel accuracy.⁹ An example of a biological problem amenable to such an approach would be the study of the conformational changes of features such as the “open” and “closed” states of ion channels. Therefore, even the pure recognition mode provides great flexibility for handling a wide array of nanobiological investigations that involve conformational changes.

The recognition system can be used in a motion tracking mode by “focusing” on a site and tracking its motion through a changing environment. In this mode, the software performs recognition of a target and creates an appropriate template for the object. The values of τ_1, τ_2 directly provide the location of the objects of each scale, which is useful for tracking. An algorithm composed of a combination of correlation and registration operations¹⁰ can be used to track the direction and magnitude of target motion. An example of a biological problem amenable to such an approach would be a receptor site investigation, since protein receptors diffuse slowly through the lipid cell membrane.

In our further research directions, we are extending the present formulation to include learning capability. A set of prototypes from each class can be stored in a prototype database as a feature vector representing the shape and surface characteristics of the object. The database of prototypes can be allowed to grow as more applications and landmarks are identified. In this way, the system “learns” the important features of the biospecimen under investigation and can do an increasingly good job in recognizing them. Beyond this, our next step will be to send appropriate motion control commands to the scanner when a feature of interest in the image has been identified for further investigation. In existing SPM systems, a nanoscale

zoom-in region is specified by means of absolute coordinates in the frame. This scheme is prone to errors due to the open loop control, locally defined origin, and false piezo activation. We are developing a new system, which is recognition driven and addresses these issues by dynamically adapting the scan coordinates to track the features of the recognized biological object.

References and Notes

1. B. Goolsby, K. Gilgenback, H. Saglik, H. Hummert, F. Salam, N. Xi, D. Wang, and V. Ayres, *Bull. Am. Phys. Soc.* 46, 1230 (2001).
2. V. Ayres, B. Goolsby, H. Hummert, N. Xi, F. Salam, K. Gilgenback, Saglik, D. Arnosti, and D. Wang, in *Abstracts of the 199th Meeting of the Electrochemical Society*, Washington, DC, March 25–30, 2001, Vol. 2001-I, No. 1144.
3. V. M. Ayres, H. Hummert, B. Goolsby, N. Xi, and F. Salam, in *Proceedings of the IEEE International Symposium on Smart Structures and Microsystems*, Hong Kong, October 19–21, 2000, pp. G1: 1-3.
4. N. Xi, F. Salam, and V. Ayres, in *NIH BECON Symposium, Nanoscience and Nanotechnology: Shaping Biomedical Research*, Bethesda, MD, June 25–26, 2000, p. 3.
5. Digital Instruments, *Nanoscope Command Reference Manual*, Chapter 10, Digital Instruments, Santa Barbara, CA.
6. Digital Instruments, *Nanoscope Command Reference Manual*, Chapter 13, Digital Instruments, Santa Barbara, CA.
7. A. L. Graps, *IEEE Comput. Sci. Eng.* 2, 50 (1995).
8. Y. Y. Tang and L. H. Yang, *Wavelet Theory and Its Application to Pattern Recognition*, World Scientific Press, Singapore (2000).
9. E. Nawapak and L. Udpa, *IEEE Trans. Image Processing* 8, 1560 (1999).
10. K. R. Castleman, *Digital Image Processing*, Prentice Hall, Englewood Cliffs, NJ (1979).

Received: 12 November 2002. Revised/Accepted: 28 March 2003.